Journal of Coordination Chemistry

ISSN: 0095-8972 (Print) 1029-0389 (Online) Journal homepage: http://www.tandfonline.com/loi/gcoo20

Thiophene-containing thiolato dimers, oxygen inserted Cu(II) complex, crystal structures, molecular docking and theoretical studies

Shaikh M. Mobin, Mohd. Tauqeer, Akbar Mohammad, Veenu Mishra & Pratibha Kumari

To cite this article: Shaikh M. Mobin, Mohd. Tauqeer, Akbar Mohammad, Veenu Mishra & Pratibha Kumari (2016) Thiophene-containing thiolato dimers, oxygen inserted Cu(II) complex, crystal structures, molecular docking and theoretical studies, Journal of Coordination Chemistry, 69:11-13, 2015-2023, DOI: 10.1080/00958972.2016.1192611

To link to this article: http://dx.doi.org/10.1080/00958972.2016.1192611

JOURNAL OF COORDINATION CHEMISTRY, 2016
VOL. 69, NOS. 11–13, 2015–2023
http://dx.doi.org/10.1080/00958972.2016.1192611

Taylor & Francis
Taylor & Francis Group

Thiophene-containing thiolato dimers, oxygen inserted Cu(II) complex, crystal structures, molecular docking and theoretical studies

Shaikh M. Mobin[a,b], Mohd. Tauqeer[c], Akbar Mohammad[a], Veenu Mishra[a] and Pratibha Kumari[b]

[a]Discipline of Chemistry, Indian Institute of Technology Indore, Indore, India; [b]Centre for Biosciences and Bio-Medical Engineering, Indian Institute of Technology Indore, Indore, India; [c]Department of Chemistry, Aligarh Muslim University, Aligarh, India

ABSTRACT

Reactions of *n*-butyl- and *n*-octyl-thiophene with CS_2 at 0 °C resulted in thiolate dimers **1** and **2**, respectively. The reaction of **1** with $Cu(NO_3)_2{\cdot}3H_2O$ in methanol under ambient reaction conditions yielded monomeric $[Cu^{II}\{(n\text{-}C_4H_9(C_4H_2S)CS_2O\}_2]$ (**3**). **1** and **3** were authenticated by their single-crystal X-ray crystal structures. Crystal structure of **3** revealed cleavage of the S-S bond of **1** followed by insertion of O-atom, forming a new five-membered Cu–O–S–C–S metallacycle. **1**, **2,** and **3** were further investigated for their bioactivity through molecular docking with nine different proteins having medicinal implications. Molecular docking of **1**, **2** and **3** revealed considerable interaction with different proteins *viz*. cancer protein Tankyrase 2, influenza viral protein Polymerase subunit PA_C–$PB1_N$ complex (H5N1), Polymerase subunit PA endonuclease (H1N1), Polymerase subunit PAn Apo(avian influenza), and FTSZ (*Bacillus subtilis*). Comparatively, **1** has promising application in therapeutics as compared to **2** and **3** based on its inhibitory constant and binding energy. Density functional theory calculations were performed to better understand the bonding of complex using MO diagram in **1–3**. Moreover, TDDFT calculations were performed to facilitate the assignment of electronic transitions of UV–Vis spectra.

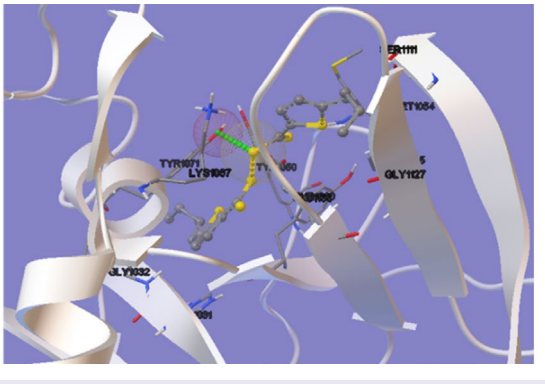

ARTICLE HISTORY
Received 18 January 2016
Accepted 5 April 2016

KEYWORDS
Thiophene-containing; oxygen inserted Cu(II) complex; crystal structure; molecular docking; DFT

CONTACT Shaikh M. Mobin xray@iiti.ac.in
Supplemental data for this article can be accessed at http://dx.doi.org/10.1080/00958972.2016.1192611.

1. Introduction

In heterocyclic compounds, thiophene is one of the most studied heterocycles, easy to process and chemically stable [1]. Thiophene increases its interest from early dye chemistry [2] to modern drug design [3], electronic and optoelectronic devices [4, 5], biodiagnostics [6], block copolymer self-assembled superstructures and conductivity-based sensory devices [7, 8]. Coordination chemistry of thiophene derivatives [9] has received attention because of its biological relevance, mainly through metal-catalyzed hydro desulfurization of fossil fuels. The 2-butylthiophene and 2-octylthiophene are used in the synthesis of anticancer and anti-atherosclerotic agents, respectively [10].

There is a growing interest in computational protein binding and virtual screening of various ligands for medicinal applications [11]. Tankyrase 2 is a promising drug target for the treatment of cancer due to its role in regulation of cell proliferation and hence it has gained attention in molecular docking studies [12]. The influenza virus is a serious public health threat due to infections leading to a large number of deaths [13]; viral polymerases are being explored searching for anti-influenza compounds [14, 15]. The effectiveness of the currently approved drugs (oseltamivir and zanamivir) is limited due to the emergence of resistant viruses; therefore, the development of new antiviral drugs is of interest [16, 17].

Cu–S bonds are of interest because of their potential applications in Michael reactions, enzymatic, desulfurization, and catalytic processes [18–21]. Insertion of a chalcogen into dithiolate-based metal complexes was first reported by Coucouvanis and Fackler where they observed the oxidation of 1,1-dithiolate ligands by the insertion of elemental sulfur leading to ring expansion in the nickel(II) complex [22]. Coucouvanis and Lippard discussed the X-ray structure of [Fe(*p*-$MeC_6H_4SC_2)_2$(*p*-$MeC_6H_4CS_3$)] which showed insertion of sulfur into a Fe–S bond [23]. Similar ring expansion where the insertion of Om instead of S was observed by Martin *et al.* in [$Cr(S_2CNR_2)_2$–(OS_2CNR_2)] [24]. X-ray structure of this complex, [$Cr(S_2CNR_2)_2$–(OS_2CNR_2)], was studied by Bond and Wallace where Cr(III) is in a pseudo-octahedral environment with two dithiocarbamate (dtc) ligands and one oxygen inserted dithioperoxycarbamate (odtc) ligand [25]. However, only two reports are known which involve the symmetric double ring expansion by insertion of oxygen in both dithiocarbamate ligands [26, 27].

Herein, we report the synthesis of 2-butylthiophene 1,1-dithiolato, **1** and 2-octylthiophene 1,1-dithiolato, **2**. Reaction of **1** with $Cu(NO_3)_2{\cdot}3H_2O$ yields mononuclear Cu(II) complex via cleavage of S–S bond and insertion of oxygen in the dithiolate ligand. The bioactivity of **1**, **2,** and **3** was assessed using molecular docking with nine different proteins. **1** revealed strong interaction with Tankyrase 2, Polymerase PA_C–$PB1_N$ complex from an avian influenza H5N1 virus and H1N1 polymerase subunit PA endonuclease. Moreover, density functional theory (DFT) and time-dependent density functional theory (TDDFT) calculations of **1–3** are also carried out to better understand the structure and electronic properties.

2. Experimental

Caution: n-Butyl lithium (*n*-BuLi) is a flammable liquid and should be handled with proper precautions.

2.1. Materials

Commercially available starting materials, thiophene, *n*-butyl lithium (*n*-BuLi), carbon disulfide (CS_2), 1-bromobutane, 1,4-dibrombutane, copper(I) bromide, hydrochloric acid (35%), $Cu(NO_3)_2{\cdot}3H_2O$, and dry solvents were used as received throughout the synthesis and reagent grade solvents were used as received. All the above-mentioned chemicals and solvents were purchased from Sigma–Aldrich/Merck India Ltd.

2.2. Physicochemical characterizations

Mass spectroscopy was performed on a Bruker Daltonik. IR analysis was done on a Fourier Transform Infrared Spectrometer, Tensor 27, BRUKER. Elemental analysis was performed on a Thermo Scientific FLASH 2000 elemental analyzer. UV–Vis spectra were measured on a Shimadzu UV-210 PC UV/

Vis spectrophotometer. Single-crystal X-ray structural studies of **1** and **3** were performed on a CCD equipped SUPERNOVA diffractometer from Agilent Technologies with Oxford Instruments low-temperature attachment.

Note: Reactions were performed under argon/nitrogen using standard Schlenk and vacuum-line techniques.

2.3. Synthesis of 1 and 2

All the reactions for the synthesis of ligands were performed under argon. Syntheses of **1** and **2** were carried out in two steps:

Step 1: To 80 mL ice cold solution of THF/hexane mixture (1 : 0.6), *n*-butyl lithium (25.0 mmol) was carefully added then 20.0 mmol thiophene was introduced dropwise at 0 °C. The solution was allowed to stand at room temperature and 1-bromobutane (20.0 mmol) or dibromobutane was added quickly and temperature of the solution was raised to 50 °C and kept at this temperature for a further half hour. Ice cold water was added to the above reaction mixture with thorough stirring. The aqueous layer was separated. Further extraction was done using diethyl ether and finally the product was dried over anhydrous $MgSO_4$. The solution was concentrated in a rotary evaporator to afford the crude product.

Step 2*:* To 80 mL ice cold solution of THF/hexane (1 : 0.6), *n*-butyl lithium (20.0 mmol) was carefully added, then 17.0 mmol of 2-butyl thiophene was introduced dropwise at 0 °C. The solution was allowed to stand at room temperature with continuous stirring. The solution was again cooled to 0 °C and a catalytic amount of copper(I) bromide was added to the reaction mixture; further dropwise addition of carbon disulfide (17.0 mmol) to the reaction mixture led to color change of red. The cooling was removed and the reaction mixture was allowed to stand at room temperature with stirring for a further 1 h. The base was quenched by addition of ice cold water and dil. HCl. Further extraction was done using diethyl ether and finally the product was dried over anhydrous $MgSO_4$. The solution was concentrated in a rotary evaporator to obtain the product. **1** and **2** were purified by column chromatography using silica gel (hexane/DCM : 9 : 1 as the eluent). Single crystal of **1** was grown in DCM/hexane mixture while we could not grow suitable single crystals of **2**.

2.4. Procedure for the synthesis of 3

A methanolic solution (40 mL) of **1** (1 mmol) was added to a solution of $Cu(NO_3)_2{\cdot}3H_2O$ (1 mmol) in methanol (20 mL) and the resultant mixture was stirred magnetically in air for 4 h at 298 K. The reaction mixture was then passed through the filter paper to remove unreacted materials. The filtrate was allowed to evaporate at room temperature for crystallization. Suitable single crystals of **3** crystallized within a week.

2.5. X-ray crystallographic determination

Single crystals of **1** and **3** were grown in DCM/hexane mixture and methanol, respectively. Single-crystal X-ray structural studies of **1** and **3** were performed on a CCD equipped SUPERNOVA diffractometer from Agilent Technologies with a low-temperature attachment. Data for **1** and **3** were collected at 150(2) K using Cu Kα radiation $\lambda_\alpha = 1.5418$ Å. The data collection was evaluated with CrysAlisPro CCD software. The data were collected by standard phi-omega scan techniques and were scaled and reduced using CrysAlisPro RED software. The structures were solved by direct methods using SHELXS-97 and refined by full matrix least squares with SHELXL-97, refining on F^2 [28].

The positions of all the atoms were obtained by direct methods. All non-hydrogen atoms were refined anisotropically. The remaining hydrogens were placed in geometrically constrained positions and refined with isotropic temperature factors, generally $1.2 \times U_{eq}$ of their parent atoms. All the H-bonding interactions, mean plane analyses, and molecular drawings were obtained using Diamond (*ver*. 2.1d). The crystal and refinement data are summarized in table 1.

Table 1. Crystal data and structure refinement for **1** and **3**.

Identification code	**1**	**3**
Empirical formula	$C_{18}H_{22}S_6$	$C_{18}H_{22}CuO_2S_6$
Formula weight	430.72	526.26
Temperature (K)	150(2)	150(2)
Color	Orange	Dark brown
Wavelength (Å)	1.5418	1.5418
Crystal system	Monoclinic	Triclinic
Space group	*C2/c*	*P* $\bar{1}$
a (Å)	16.7354(4)	8.5519(6)
b (Å)	5.44410(10)	9.3688(5)
c (Å)	22.5140(5)	14.2628(10)
α (°)	90	77.583(5)
β (°)	91.504(2)	86.424(5)
γ (°)	90	85.142(5)
Volume (A^3)	2050.53(8)	1110.87(13)
Z	4	2
d_{Calcd} (mg m^{-3})	1.395	1.573
μ (mm^{-1})	6.136	6.757
F(0 0 0)	904	542
Crystal size (mm^3)	0.33 × 0.26 × 0.21	0.33 × 0.28 × 0.22
θ range (°)	5.29–71.95	3.18–72.37
Index ranges	$-20 \le h \le 20, -6 \le k \le 3, -27 \le l \le 26$	$-7 \le h \le 10, -11 \le k \le 11, -17 \le l \le 17$
Reflections collected/unique	6175/1994 [*R*(int) = 0.0186]	7671/4257 [*R*(int) = 0.0214]
Absorption correction	Semi-empirical from equivalents	Semi-empirical from equivalents
Max. and min. transmission	0.3590 and 0.2367	0.3179 and 0.2139
Refinement method	Full-matrix least-squares on F^2	Full-matrix least-squares on F^2
Data/restraints/parameters	1994/0/110	4257/0/246
GOF, F^2	1.041	1.072
R_1, wR_2 [$I > 2\sigma(I)$]	$R_1 = 0.0265$, $wR_2 = 0.0712$	$R_1 = 0.0483$, $wR_2 = 0.1283$
R_1, wR_2 (all data)	$R_1 = 0.0277$, $wR_2 = 0.0724$	$R_1 = 0.0632$, $wR_2 = 0.1435$
Largest diff. peak and hole (e $Å^{-3}$)	0.317 and −0.304	0.675 and −0.495
CCDC No.	1038191	1038193

2.6. Spectroscopic data for 1, 2 and 3

1: MS (*m/z*, ES^+): M + Na = 453; IR (KBr, cm^{-1}): 2927(s), 1432(s), 1346(m), 1200(s), 1047(s), 938(m), 790(s), 654 (m). Anal. Calcd (%): C, 50.19; H, 5.15; S, 44.66. Found (%): C, 50.55; H, 5.09; S, 44.32. Yield: 295 mg, 58%.

2: MS (*m/z*, ES^+): M + Na = 565; IR (KBr, cm^{-1}): 2925(s), 1443(s), 1341(m), 1202(s), 1048(m), 927(w), 798(s), 657 (m). Anal. Calcd (%): C, 57.51; H, 7.05; S, 35.43. Found (%): C, 57.17; H, 7.24; S, 35.17. Yield: 139 mg, 21.5%.

3: MS (*m/z*, ES^+): M-((C_4H_2S)C_4H_9) = 387; IR (KBr, cm^{-1}): 2926(s), 1452(s), 1368(m), 1202(s), 1093(s), 996(w), 749(s), 647(m). Anal. Calcd (%): C, 41.08; H, 4.21; O, 6.08; S, 36.56. Found (%): C, 40.70; H, 4.84; O, 6.55; S, 36.06. Yield: 83 mg, 68%.

2.7. Molecular docking

The bioactivities of **1**, **2,** and **3** were analyzed using molecular docking with different proteins. Nine protein structures were downloaded from the Protein Data Bank (http://www.rcsb.org/pdb). The studied proteins were Tankyrase 2, Polymerase PA_C–$PB1_N$ complex from an avian influenza H5N1 virus, H1N1 polymerase subunit PA endonuclease, avian influenza virus PAn Apo, TypeIII Pantothenate Kinase (CoaX) from Bacillus Anthracis, Hepatitis C virus NS5B polymerase, FTSZ *Bacillus subtilis*, HIV-1 integrase and SepF-like protein from Pyrococcusfuriosus.

All water molecules were deleted and polar hydrogens were added to all the proteins. After that Kollman and Gastegier charges were assigned; rotatable bonds of ligands were set to rotate. The grid parameter file of each protein was generated by MGL AutoDock Tool. A huge grid-box was created to cover entire protein domains. The center of the protein structure was used as the center of the grid-box. The spacing between grid points was set as default value of 0.375 Å. The docking of ligands

with protein was done using AutoDock4.2 [29]. All calculations of docking were performed using the Lamarckian Genetic Algorithm method. The maximum number of generations was set to 27,000 and maximum number of top individuals that automatically survived was set to 1 with mutation rate of 0.02, crossover rate of 0.8. The same parameters were used for all proteins. After performing docking, 10 conformations were generated. The best conformation was selected with the minimum binding energy and inhibitory constant.

2.8. Computational details

DFT calculations were performed using the Gaussian 09 code [30]. We employed dispersion corrected B3LYP-D2 functional for the structural optimization [31]. The B3LYP-D2 functional has a proven track record of predicting the correct structures [32–36]. The TZYP basis set for copper (Cu) and sulfur (S) and a 6–31G* basis set for carbon hydrogen and oxygen have been employed throughout the calculations [36–44]. The electronic excitations were obtained from for TDDFT calculations at the same level of theory [37, 45]. All structures studied in this article were fully optimized as gas-phase without any restriction. We believe such basis sets are sufficient for accurate DFT calculations.

3. Results and discussion

3.1. Synthesis

Compounds **1** and **2** were obtained by slight modification of literature synthetic procedure [46] (scheme 1). Unlike **1**, in **2** the self-coupling of the butyl group led to formation of an eight-membered aliphatic octyl chain. Complex **3** was obtained on addition of $Cu(NO_3)_2{\cdot}3H_2O$ to a methanolic solution of **1** at 298 K (scheme 2). The formation of **3** from **1** involves two simultaneously operating important chemical processes: (i) cleavage of S–S bond of **1** and (ii) insertion of oxygen into the copper-sulfur bond, forming a new S-O bond [24–27], which has been authenticated by single-crystal X-ray structure of **3** (see later). However, **2** failed to react with $Cu(NO_3)_2{\cdot}3H_2O$ under identical reaction conditions.

Compounds **1**, **2,** and **3** were characterized using mass and IR spectroscopies and elemental analyses. Single crystals of **1** and **3** were grown from dichloromethane/hexane mixtures and methanol, respectively, and their structures were established by X-ray crystallographic studies.

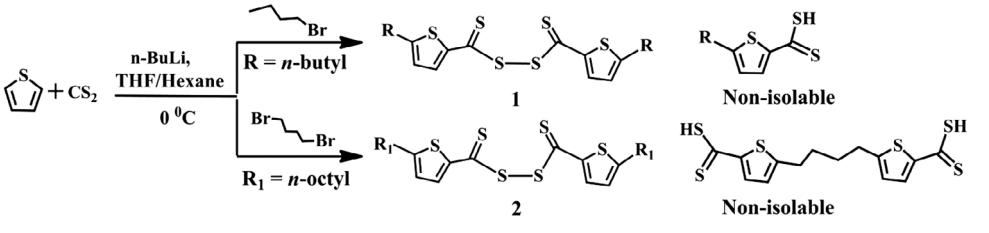

Scheme 1. Synthesis of **1** and **2**.

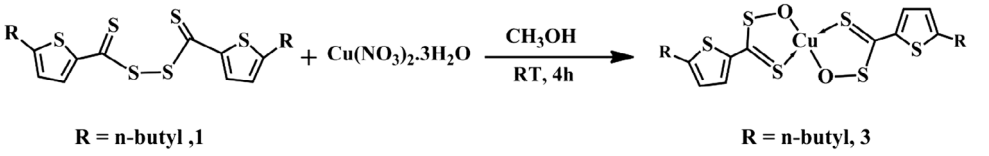

Scheme 2. Synthesis of **3**.

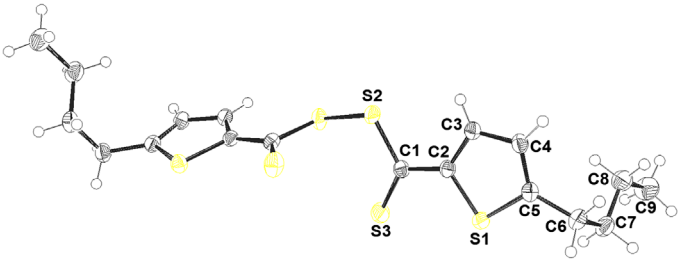

Figure 1. ORTEP view of **1** at 50% probability.

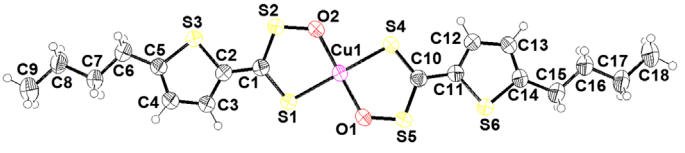

Figure 2. ORTEP view of **3** at 50% probability.

3.2. Description of crystal structures

1 crystallizes in the monoclinic *C2/c* space group with a crystallographically imposed inversion center (figure 1, table 1). Molecular structure of **1** has the side chain which contains four aliphatic carbons attached to the thiophene units, and appeared in a *zig-zag* fashion.

The packing diagram of **1** reveals the presence of weak intermolecular C–H···S and C-H···π interactions. The C–H···S interaction involving hydrogen of methylene (CH_2) and sulfur of an adjacent unit C(6)–H(6B)···S(3) 2.954 Å and C–H···π interactions exist between C of thiophene and adjacent H of another thiophene C(3)–H(3)···C(3) 2.824(1) Å, leading to a 1-D polymeric chain (figure S1, table S1). This further extends via C(6)–H(6B)···S(3) 2.954 Å interaction, yielding a 2-D-network along the *c*-axis (figure S2).

3 crystallizes in the triclinic *P* $\bar{1}$ space group (figure 2, table 1). Cu(II) in [Cu{(nC_4H_9)(C_4H_2S)CS_2O}$_2$] (**3**) is in S_2O_2 coordination environment with bond distances of Cu(1)–O(1), 1.929(2) Å, Cu(1)–O(2),1.923(3) Å, Cu(1)–S(1), 2.259(8) Å, Cu(1)–S(4), 2.262(2) Å and bond angles O(1)–Cu(1)–S(4), 90.48(7)°, O(2)–Cu(1)–S(1), 90.36(7)°, O(1)–Cu(1)–S(1), 89.6(7)° and O(2)–Cu(1)–S(4), 89.58(7)°, which suggests distorted square planar geometry around Cu(II). The C–S distances of CS_2 moieties are 1.669(3) and 1.693(3) Å, consistent with delocalization of the double bond of the related complexes [37, 47–51].

The packing of **3** reveals the presence of weak intermolecular C–H···O and C–H···S hydrogen bonding interactions. The intermolecular C–H···O and C–H···S hydrogen bonds involve two H-atoms of thiophene from one layer to O and S from adjacent layers (C(4)-H(4)···O(2) 2.719(2) Å, C(13)–H(13)···O(1) 2.705(2) Å) and (C(3)–H(3)···S(4) 2.935(1) Å and C(12)–H(12)···S(1) 2.955(1) Å), which continues along the *c*-axis forming a1-D-polymeric chain (figure S3, table S2).

The formation of **3** under atmospheric reaction conditions (see Section 2) can tentatively be interpreted by the metal mediated cleavage of the S–S bond [52] of preformed **1**, yielding the dithiolato coordinated intermediate [Cu^{II}{(*n*-C_4H_9)(C_4H_2S)CS_2}$_2$], followed by insertion of oxygen into both Cu–S– bonds [26, 27] to form Cu–O–S– linkages in **3**. To the best of our knowledge, only two reports on this sort of double ring expansion are known where oxygen is inserted in both thiolate units: (i) [$Et_2In(OS_2CNMenBu)]_2$ is prepared serendipitously by exposure of [$In(S_2CNMenBu)_3$] and triethylindium solution in air [26] and (ii) $Zn(O\text{-}deDTC)_2$ (DTC = a disulfide derivative of *N*,*N*-diethyl dithiocarbamate) is obtained by initial reaction of the DTC salt with stoichiometric oxidant prior to its complexation with Zn(II) [27].

3.3. Molecular docking studies

In order to characterize bioactivity of potentially active compounds by molecular docking, nine proteins were selected and their structures were collected from protein data bank. The docking studies were performed using AutoDock 4.2 [53]. The proteins were ranked on the basis of their binding affinity with **1**, **2,** and **3**. Three target proteins with high binding affinity towards **1**, **2,** and **3** are demonstrated in table S3 and the rest are exhibited in table S4. It is evident from tables S3 and S4 that **1** has better binding than **2** and **3** with all the studied proteins. **1** revealed strong interaction with Tankyrase 2 (cancer protein), Polymerase PA_C–$PB1_N$ (H5N1 virus), and Polymerase subunit PA endonuclease (H1N1 virus). Figures S4–S6 demonstrate the 2-D and 3-D binding conformations of **1**, **2,** and **3**, respectively, with various protein molecules. The inhibition constant of **1** toward H1N1 polymerase subunit PA endonuclease is better than a recently reported compound [54], which makes **1** a potential candidate for anti-influenza therapy in the era of emergence of drug-resistant virus.

3.4. DFT studies

In order to further understand the bonding of **1**–**3**, DFT calculations were performed (figure S7a, S7b, S7c and table S5a and S5b). The DFT optimized geometry and structural parameters of **1** and **3** nearly match the experimental results (table S5(a)).

Selected Highest Occupied Molecular Orbitals (HOMO) of **3** have been analyzed using DFT calculations to unfold interactions around Cu(II) (figure S8). The significant interactions of d-orbitals of copper and p-orbitals of oxygen and sulfur are reflected in HOMO-8, HOMO-28, HOMO-30, and HOMO-35, respectively.

The experimental and TDDFT calculated electronic spectral profiles of **1**–**3** in CH_2Cl_2 are shown in figure S9(i), S9(ii) and the data are listed in table S6. **1**–**3** exhibit moderately intense multiple transitions in the UV–Vis region and TD-DFT calculations based on the DFT optimized structures of **1**–**3** (figure S10(A)–(C)) facilitate the assignment of the experimental transitions. The different bands for **1** at 379 nm (DFT: 346 nm), 305 nm (DFT 302 nm) and 254 nm (DFT: 255 nm) and for **2** at 378 nm (DFT: 339 nm), 312 nm (DFT 303 nm) and 261 nm (DFT: 256 nm) are assigned to intra-ligand transitions (thiophene-1,1-dithiolato → thiophene 1,1-dithiolato), as shown in figure S10(A) and (B) and table S6. The observed peak at 403 nm (DFT: 423 nm) for **3** is attributed to ligand to metal charge transfer transition (HOMO-7 to HOMO). The intra-ligand higher energy UV transitions at 343 nm (DFT: 353 nm), 282 nm (DFT: 308 nm) and 254 nm (DFT: 285 nm) involve HOMO-1 to LUMO, HOMO-4 to LUMO and HOMO-6 to LUMO based transitions, respectively (figure S10(C), table S6).

4. Conclusion

The present article demonstrates the formation of copper mediated simultaneous S–S bond cleavage of preformed **1** as well as insertion of oxygen into the Cu–S bond leading to a new Cu–O–S linkage in square planar Cu(II) complex **3**. Investigation of molecular docking of **1**, **2** and **3** revealed that **1** has relatively strong binding with medicinal proteins. On the basis of computational studies, the effectiveness of **1**, in terms of inhibition constant, reveals it as a candidate for a potential influenza drug, which will be further explored experimentally. Theoretical investigation further supports the structural and electronic properties of the studied compounds.

Supplementary material

Other figures and tables are shown in supporting information. Crystallographic data for the structural analysis have been deposited with the Cambridge Crystallographic Data Center, CCDC no.'s 1038191 and 1038193 for **1** and **3**, respectively.

Acknowledgements

S.M.M. would like to acknowledge CSIR, New Delhi, India for funding. We sincerely acknowledge Sophisticated Instrumentation Centre (SIC), IIT Indore for providing the characterization facility. A.M. and P.K. would like to thank to MHRD New Delhi, Govt. of India for providing the fellowship. We also gratefully acknowledge Prof. G. Rajaraman and A. Ansari from IIT Bombay for their helpful discussion on DFT studies.

Disclosure statement

No potential conflict of interest was reported by the authors.

References

[1] G. Barbarella, M. Melucci, G. Sotgiu. *Adv. Mater.*, **17**, 1581 (2005).
[2] W.J. King, F.F. Nord. *J. Org. Chem.*, **14**, 638 (1949).
[3] C. Wu, E.R. Decker, N. Blok, H. Bui, T.J. You, J. Wang, A.R. Bourgoyne, V. Knowles, K.L. Berens, G.W. Holland, T.A. Brock, R.A.F. Dixon. *J. Med. Chem.*, **47**, 1969 (2004).
[4] M. Halik, H. Klauk, U. Zschieschang, G. Schmid, S. Ponomarenko, S. Kirchmeyer, W. Weber. *Adv. Mater.*, **15**, 917 (2003).
[5] C. Rost, S. Karg, W. Riess, M.A. Loi, M. Murgia, M. Muccini. *Appl. Phys. Lett.*, **85**, 1613 (2004).
[6] K. Doré, S. Dubus, H.A. Ho, I. Lévesque, M. Brunette, G. Corbeil, M. Boissinot, G. Boivin, M.G. Bergeron, D. Boudreau, M. Leclerc. *J. Am. Chem. Soc.*, **126**, 4244 (2004).
[7] D.M. Vriezema, J. Hoogboom, K. Velonia, K. Takazawa, P.C.M. Christianen, J.C. Maan, A.E. Rowan, R.J.M. Nolte. *Angew. Chem. Int. Ed.*, **42**, 772 (2003).
[8] H. Yu, A.E. Pullen, M.G. Büschel, T.M. Swager. *Angew. Chem. Int. Ed.*, **43**, 3700 (2004).
[9] B.C. Gates, J.R. Katzer, G.C.A. Schuit. *Chemistry of Catalytic Processes*., McGraw-Hill, New York (1979).
[10] R. Mishra, K.K. Jha, S. Kumar, I. Tomar. *Der PharmaChemica*, **3**, 38 (2011).
[11] P. Pradeep, C. Struble, T. Neumann, D.S. Sem, S.J. Merrill. *IEEE/ACM Trans. Comput. Biol. Bioinf.*, **12**, 1464 (2015).
[12] M. Narwal, J. Koivunen, T. Haikarainen, E. Obaji, O.E. Legala, H. Venkannagari, P. Joensuu, T. Pihlajaniemi, L. Lehtiö. *J. Med. Chem.*, **56**, 7880 (2013).
[13] S.A. Harper, J.S. Bradley, J.A. Englund, T.M. File, S. Gravenstein, F.G. Hayden, A.J. McGeer, K.M. Neuzil, A.T. Pavia, M.L. Tapper, T.M. Uyeki, R.K. Zimmerman. *Clin. Infect. Dis.*, **48**, 1003 (2009).
[14] C. Tintori, I. Laurenzana, A.L. Fallacara, U. Kessler, B. Pilger, L. Stergiou, M. Botta. *Bioorg. Med. Chem. Lett.*, **24**, 280 (2014).
[15] S. Massari, G. Nannetti, L. Goracci, L. Sancineto, G. Muratore, S. Sabatini, G. Manfroni, B. Mercorelli, V. Cecchetti, M. Facchini, G. Palù, G. Cruciani, A. Loregian, O. Tabarrini. *J. Med. Chem.*, **56**, 10118 (2013).
[16] S. Pautus, P. Sehr, J. Lewis, A. Fortuné, A. Wolkerstorfer, O. Szolar, D. Guilligay, T. Lunardi, J.L. Décout, S. Cusack. *Chem. Lett.*, **56**, 8915 (2013).
[17] Y. Hu, S. Lu, Z. Song, W. Wang, P. Hao, J. Li, X. Zhang, H.L. Yen, B. Shi, T. Li, W. Guan, L. Xu, Y. Liu, S. Wang, X. Zhang, D. Tian, Z. Zhu, J. He, K. Huang, H. Chen, L. Zheng, X. Li, J. Ping, B. Kang, X. Xi, L. Zha, Y. Li, Z. Zhang, M. Peiris. *Lancet*, **381**, 2273 (2013).
[18] (a) Y. Lu. In *Bio-coordination Chemistry*, L. Que, Jr. W.B. Tolman (Eds.), Vol. 8, p. 91, Elsevier, Oxford (2004); (b) P. Chen, S.I. Gorelsky, S. Ghosh, E.I. Solomon. *Angew. Chem., Int. Ed.*, **43**, 4132 (2004); (c) Y. Lee, A.A.N. Sarjeant, K.D. Karlin. *Chem. Commun.*, 621 (2006); (d) E.I. Solomon, R.K. Szilagyi, S.D. George, L. Basumallick. *Chem. Rev.*, **104**, 419 (2004); (e) D.B. Rorabacher. *Chem. Rev.*, **104**, 651 (2004); (f) J.T. York, I. Bar-Nahum, W.B. Tolman. *Inorg. Chim. Acta*, **361**, 885 (2008).
[19] H. Pellissier. *Chiral Sulfur Ligands: Asymmetric Catalysis*, Vol. 93, RSC, Cambridge (2009).
[20] (a) W.H. Tian, L.B. Sun, X.L. Song, X.Q. Liu, Y. Yin, G.S. He. *Langmuir*, **26**, 17398 (2010); (b) P. Baeza, G. Aguila, F. Gracia, P. Araya. *Catal. Commun.*, **9**, 751 (2008); (c) A.J. Hernández-Maldonado, F.H. Yang, G. Qi, R.T. Yang. *Appl. Catal., B*, **56**, 111 (2005).
[21] (a) S. Fumitoshi, M. Toshiaki, S. Aiko. *Nipp. Kag. Koe. Yok.*, **84**, 739 (2004); (b) S. Fumitoshi, Y. Atsunori, S. Aiko, M. Toshiaki. *Nipp. Kag. Koe. Yok.*, **86**, 1006 (2006).
[22] D. Coucouvanis, J.P. Fackler Jr. *J. Am. Chem. Soc.*, **89**, 1346 (1967).
[23] (a) D. Coucouvanis, S.J. Lippard. *J. Am. Chem. Soc.*, **90**, 3281 (1968); (b) D. Coucouvanis, S.J. Lippard. *J. Am. Chem. Soc.*, **91**, 307 (1969).
[24] J.M. Hope, R.L. Martin, D. Taylor, A.H. White. *J. Chem. Soc., Chem. Commun.*, 99, (1977).
[25] A.M. Bond, G.J. Wallace. *Inorg. Chem.*, **23**, 1858 (1984).
[26] M.A. Malik, M. Afzaal, P. O'Brien, M. Halliwell. *Polyhedron*, **25**, 864 (2006).
[27] D.F. Brayton, K. Tanabe, M. Khiterer, K. Kolahi, J. Ziller, J Greaves, P.J. Farmer. *Inorg. Chem.*, **45**, 6064 (2006).
[28] G.M. Sheldrick, *Acta Crystallogr.*, **A64**, 112 (2008). *Program for Crystal Structure Solution and Refinement*, University of Gottingen, Gottingen, Germany (1997).
[29] G.M. Morris, R. Huey, W. Lindstrom, M.F. Sanner, R.K. Belew, D.S. Goodsell, A.J. Olson. *J. Comput. Chem.*, **30**, 2785 (2009).

[30] M.J. Frisch, G.W. Trucks, H.B. Schlegel, G.E. Scuseria, M.A. Robb, J.R. Cheeseman, G. Scalmani, V. Barone, B. Mennucci, G.A. Petersson, H. Nakatsuji, M. Caricato, X. Li, H.P. Hratchian, A.F. Izmaylov, J. Bloino, G. Zheng, J.L. Sonnenberg, M. Hada, M. Ehara, K. Toyota, R. Fukuda, J. Hasegawa, M. Ishida, T. Nakajima, Y. Honda, O. Kitao, H. Nakai, T. Vreven, J.A. Montgomery Jr., J.E. Peralta, F. Ogliaro, M. Bearpark, J.J. Heyd, E. Brothers, K.N. Kudin, V.N. Staroverov, R. Kobayashi, J. Normand, K. Raghavachari, A. Rendell, J.C. Burant, S.S. Iyengar, J. Tomasi, M. Cossi, N. Rega, J.M. Millam, M. Klene, J.E. Knox, J.B. Cross, V. Bakken, C. Adamo, J. Jaramillo, R. Gomperts, R.E. Stratmann, O. Yazyev, A.J. Austin, R. Cammi, C. Pomelli, J.W. Ochterski, R.L. Martin, K. Morokuma, V.G. Zakrzewski, G.A. Voth, P. Salvador, J.J. Dannenberg, S. Dapprich, A.D. Daniels, Ö. Farkas, J.B. Foresman, J.V. Ortiz, J. Cioslowski, D.J. Fox, *GAUSSIAN 09* (2009) (Revision A.1), Gaussian, Inc., Wallingford, CT.
[31] S. Grimme. *J. Comput. Chem.*, **27**, 1787 (2006).
[32] A. Ansari, A. Kaushik, G. Rajaraman. *J. Am. Chem. Soc.*, **135**, 4235 (2013).
[33] A. Bassan, M.R.A. Blomberg, P.E.M. Siegbahn, L. Que Jr. *Angew. Chem. Int. Ed.*, **44**, 2939 (2005).
[34] P.E.M. Siegbahn. *J. Biol. Inorg. Chem.*, **11**, 695 (2006).
[35] P. Mathur, M. Tauqeer, R.S. Ji, D.K. Rai, S.M. Mobin, G.K. Lahiri. *J. Cluster Sci.*, **26**, 157 (2015).
[36] M. Ansari, N. Vyas, A. Ansari, G. Rajaraman. *Dalton Trans.*, **44**, 15232 (2015).
[37] S. Singh, J. Chaturvedi, S. Bhattacharya. *Dalton Trans.*, **41**, 424 (2012).
[38] T.H. Dunning Jr., P.J. Hay. *Modern Theoretical Chemistry*, **3**, 1 (1976).
[39] P.J. Hay, W.R. Wadt. *Chem. Phys.*, **82**, 270 (1985).
[40] P.J. Hay, W.R. Wadt. *Chem. Phys.*, **82**, 299 (1985).
[41] P.J. Hay, W.R. Wadt. *Chem. Phys.*, **82**, 284 (1985).
[42] R. Ditchfield, W.J. Hehre, J.A. Pople. *J. Chem. Phys.*, **54**, 724 (1971).
[43] A. Schäfer, H. Horn, R. Ahlrichs. *J. Chem. Phys.*, **97**, 2571 (1992).
[44] A. Schäfer, C. Huber, R. Ahlrichs. *J. Chem. Phys.*, **100**, 5829 (1994).
[45] J. Tomasi, B. Mennucci, E. Cancès. *J. Mol. Struct. (Thoechem)*, **464**, 211 (1999).
[46] M.S. Thomas, M. Landman, S. Lotz, E.M. van der Merwe. *Polyhedron*, **26**, 3471 (2007).
[47] A.M. Manotti Lanfredi, F. Ugozzoli, F. Asaro, G. Pellizer, N. Marsich, A. Camus. *Inorg. Chim. Acta*, **192**, 271 (1992).
[48] A. Camus, N. Marsich, A.M.M. Lanfredi, F. Ugozzoli. *Inorg. Chim. Acta*, **161**, 89 (1989).
[49] (a) W.G. Weber, J.B. McLeary, R.D. Sanderson. *Tetrahedron Lett.*, **47**, 4771 (2006); (b) O. Niyomura, Y. Kitoh, K. Nagayama, S. Kato. *Sulfur Lett.*, **22**, 195 (1999).
[50] H. Wu, C.R. Lucas. *Inorg. Chem.*, **3**, 526 (1992).
[51] A.E. Pullen, S. Zeltner, R.-M. Olk, E. Hoyer, K.A. Abboud, J.R. Reynolds. *Inorg. Chem.*, **35**, 4420 (1996).
[52] L. Han, X. Bu, Q. Zhang, P. Feng. *Inorg. Chem.*, **45**, 5736 (2006).
[53] G.M. Morris, D.S. Goodsell, R.S. Halliday, R. Huey, W.E. Hart, R.K. Belew, A.J. Olson. *J. Comput. Chem.*, **19**, 1639 (1998).
[54] S. Fudo, N. Yamamoto, M. Nukaga, T. Odagiri, M. Tashiro, S. Neya, T. Hoshino. *Bioorg. Med. Chem.*, **23**, 5466 (2015).